Journal of Engg. Research Vol. 7 No. (3) September 2019 pp. 76-89

Study on bearing capacity characteristics of rock socketed short pile in weathered rock site

Li Xin-yuan*, Bai Xiao-yu and Zhang Ming-yi

**School of Civil Engineering, Xuzhou University of Technology, Xuzhou, 221018, China*
College of Civil Engineering, Qingdao University of Technology, Qingdao, 266033, China
**Corresponding Author: lixy.qtech@live.com*

ABSTRACT

The bearing behaviour and load transfer mechanism of the rock socketed short pile were studied by the test and FEM of two different cases of 11 single short piles in a weathered rock foundation in Qingdao. The influences of aspect ratio and rock socketed length on the bearing behaviours of rock socketed short piles were discussed by FEM. The results show that the ultimate bearing capacity of rock socketed short piles is higher, and settlement is smaller, which means that they can satisfy the engineering demands and have high security reserves. Moreover, a change in the ultimate bearing capacity is not easily noticed with increasing of pile lengths, which demonstrates that the 11 piles have strong end bearing properties. The pile side friction peak decreases with an increase of the aspect ratio, as does the pile top settlement. Under different rock socketed lengths, the attenuation law of axial force is consistent; the pile top settlement decreases with the increase of rock-socketed length, and the ratio of base resistances to the bearing capacities decreases with the increase of the length. The research results can provide references for rock socketed short pile design in similar geological conditions.

Keywords: bearing behaviour; in situ test; rock socketed short pile; strong weathered granite; ultimate bearing capacity.

INTRODUCTION

Granite is widely distributed in Qingdao, China. Granite has the unique characteristics of a great difference in the degree of weathering, as well as a great variation in its buried depth (Madhusudhan et al., 2017). This characteristic leads to a situation that the length of a pile varies greatly while the distance between adjacent piles is very small. This situation is often encountered in designing pile foundation on weathered granite (Cho et al., 2014). Most designs tend to increase the length of the pile on the higher bed rock, rather than adjusting the length of the pile according to the undulation of bedrock. This greatly increases the difficulty in construction (Musarra et al., 2015). Blasting excavation methods that resulted in a decrease of the bearing capacity were often used (Xia et al., 2013). At present, the bearing mechanism of short piles is not fully understood by engineers, and no definite design basis and method have been issued (Kwon et al., 2014). The short piles were used with great caution or not adopted at all. The advantage of this technique is that the pile and bed rock are not fully used. Thus, finding a reasonable design method and characterizing the bearing potential of rock socketed short piles are urgent problems to be solved. Considerable research is available in the literature concerning the problem of the bearing capacity of rock socketed piles. Rowe (1987) studied the influence of different test methods (including the displacement control method and the load control method) on the ultimate value of the side friction. Leong (1994) observed that the side friction of the pile decreases slightly with an increase in the draw ratio. Hassan (1997) found that the dilatancy angle of the bedrock has less influence on the side friction of the pile. Armaghani et al. (2016) presented a new model for predicting the settlement of the rock-socketed pile.

Two related tests were carried out in this paper: (1) A static loading test of a PHC (high strength prestressed concrete) pipe pile on strong weathered rock, in which the ultimate bearing capacity of single PHC pipe pile is explored from the perspective of load and deformation, which is compared to bored piles on the same strong weathered granite;

(2) A static loading test of a large diameter rock socketed short pile on strongly weathered granite. Based on the static loading tests, the bearing behaviour of socketed short piles in strongly weathered granite is analysed, and the influence factors of bearing capacity are studied using the finite element method.

GENERAL SITUATION AND SCHEME OF THE TEST

Test 1: Static Loading Test of PHC Pipe Pile on Strong Weathered Rock

The project is located in the Qingdao power plant. Both the PHC pipe piles and the artificial dig hole piles were adopted in the same project, which is good for contrastive analysis. Figure1 shows the PHC pipe piles and the cast-in-place piles at the test site. The physical and mechanical parameters of the soil and rock are shown in Table 1.

(a) PHC pipe piles and bored piles

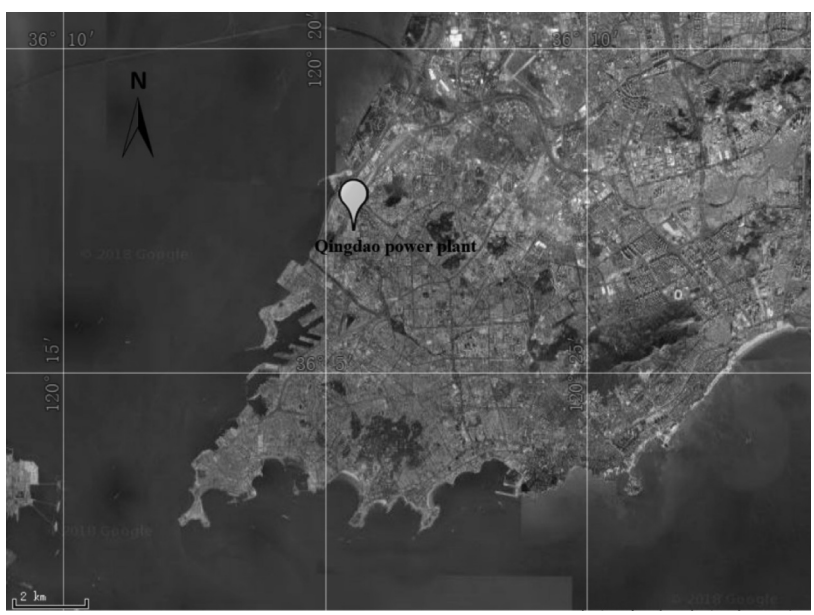

(b) The location of Qingdao power plant

Fig. 1. PHC pipe piles and bored piles in situ.

Table 1. Physical and mechanical parameters.

Soil	Thickness /m	Modulus of elasticity /MPa	Characteristic value of bearing capacity /kPa
Miscellaneous fill	0.60 - 3.00	5.0	
Rinse fill	0.50 - 2.80	6.0	160
Qpal	0.50 - 3.00	7.6	250
Strongly weathered granite	3.50 - 5.10	40.0	1000
Moderately weathered granite	3.70 - 4.80	3300	2000

The diameter of PHC pipe piles is 0.55m, while the thickness of the wall is 0.12m, the strength grade of concrete is C80, the pile tip is embedded into the strongly weathered granite approximately 0.5m deep, and the pipes are constructed by the hammer method. The vertical ultimate bearing capacity is estimated as 3MN. The diameter of the artificial bored pile is 0.80m, the strength grade of concrete is C30, the water-cement ratio is 0.45, and the thickness of the reinforced concrete protection layer is 60mm. The vertical ultimate bearing capacity is determined by the loading test. Table 2 shows the parameters of testing piles.

Table 2. Parameters of testing piles.

No.	Pile type	Diameter /m	Length /m	Aspect ratio(L/D)
TP1	PHC	0.55	6.5	11.82
TP2	PHC	0.55	7.0	12.73
TP3	PHC	0.55	6.5	11.82
TP4	PHC	0.55	7.0	12.73
TP5	PHC	0.55	7.0	12.73
TP6	artificial dig hole piles	0.80	7.2	9.00
TP7	artificial dig hole piles	0.80	6.6	8.25

The surcharge-reaction beam system loading was employed for this test, and the slow loading method was adopted. The settlement was obtained by the 4 symmetrically arranged dial gauges. The reading time, termination test conditions, and determination of the ultimate bearing capacity were performed in accordance with the specifications.

Test 2: Static Loading Test of Rock Socketed Short Pile on Strongly Weathered Granite

The project is located in the Shibei District Qingdao City. The formation of the whole field is simple. The field is a complex stratum of soil and rock, and the main physical and mechanical parameters of each soil and rock layer are shown in Table 3.

Table 3. Physical and mechanical parameters.

Soil	Thickness /m	Modulus of elasticity /MPa	Characteristic value of bearing capacity /kPa
Miscellaneous fill	0.40 - 6.20	5.0	
Medium sand	0.50 - 5.10	16.0	160
Silty clay	0.50 - 8.20	12.0	220
Coarse sand	1.00 - 8.90	25.0	220
Strongly weathered granite	0.40 - 9.20	46.0	1000
Moderately weathered granite		3500.0	2200

Bored piles with large diameters and unequal lengths were adopted in this project. The rock socketed depth is 1.0*D* (where *D* is the pile diameter), the strength grade of concrete is C30, and the vertical ultimate bearing capacity is estimated to be 3500kN (when the diameter of the pile is 0.80m) and 4450kN (when the diameter of the pile 0.90m). The parameters of the testing pile are shown in Table 4.

Table 4. Parameters of testing piles.

No.	Pile type	Diameter /m	Length /m	Rock socketed depth /m	Aspect ratio
TP8	artificial dig hole piles	0.9	6.59	0.9	7.32
TP9	artificial dig hole piles	0.8	5.78	0.8	7.23
TP10	artificial dig hole piles	0.8	2.52	0.8	3.15
TP11	artificial dig hole piles	0.9	2.18	0.9	2.42

The test method in this experiment is exactly the same as that of experiment 1.

TEST 1 RESULTS AND ANALYSIS

The load transfer behaviour, pile-soil interaction law, and the failure model can be derived for the load - settlement (Q - s) curve. The overall grasp of the behaviour of a pile can be achieved by analysis of the Q - s curve. The Q - s curves of 7 piles in the test area are shown in Figure 2, while the static loading test results are shown in Table 5, where the springback is the instantaneous recovery deformation at the time of unloading and the residual settlement is an unrecoverable settlement; its value is the difference between settlement of pile head and springback.

It can be observed from Figure 2 that all of the 5 Q - s curves of the PHC pipe pile show a slowly changing shape, with the settlement of the pile top being quite small (< 8 mm), even when the load is very large (the load is approximately 3MN). This finding means that the bearing capacity satisfies the design requirements. Combined with Table 5, this result shows that the residual ratio of settlement of the pile top of TP1 - TP5 is between 80% and 89%, the rebound settlement is not large, and the rebound ratio is between 11% and 20%. This finding means that the elastic characteristic of pile is not obvious. The reason is that the bedrock produced an irreversible plastic deformation when the load level was high. The rebound of the pile top also shows that the rock socketed PHC pipe pile has end-bearing characteristics.

TP6 and TP7 have not entered the failure stage during the loading process. When the load is 10MN, the settlement of the pile top is less than 32mm, and the residual ratios of settlement of pile top were 70.5% and 73.8%; the rebound rate is almost 2 times that of the PHC pipe pile.

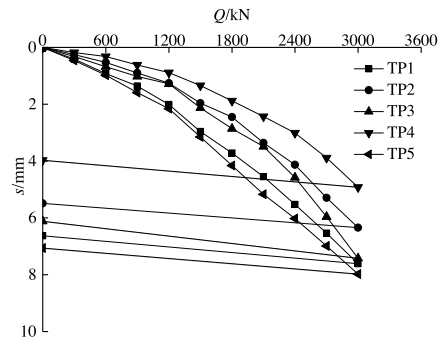

(a) PHC piles

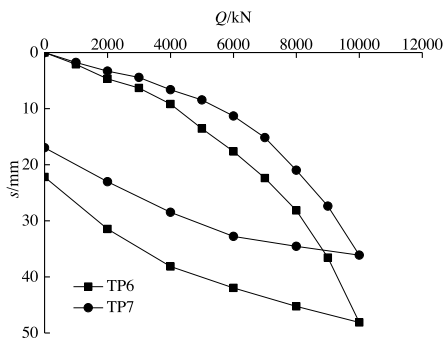

(b) artificial dig hole piles

Fig. 2. Load-displacement curves for static loading tests.

Table 5. Results of compressive static loading tests.

No.	Maximum load /kN	Settlement of pile head /mm	Springback / mm	Residual settlement /mm	Rebound ratio /%	The proportion of residual settlement to total settlement /%
TP1	3000	7.61	0.98	6.63	12.9	87.1
TP2	3000	6.34	0.85	5.49	13.4	86.6
TP3	3000	7.42	1.30	6.12	17.5	82.5
TP4	3000	4.92	0.95	3.97	19.3	80.7
TP5	3000	7.98	0.92	7.06	11.5	88.5
TP6	10000	31.46	9.27	22.19	29.5	70.5
TP7	10000	23.02	6.04	16.98	26.2	73.8

TEST 2 RESULTS AND ANALYSIS

Compressive Static Loading Test Results

The *Q* - *s* curves of 4 piles in the test area are shown in Figure 3, while the static loading test results are shown in Table 6. Figure 3 shows that all the 4 piles have not entered the failure stage during the loading process. *Q* - *s* curves show a slowly changing shape, which implies that the settlement of the pile top is notably small (<25 mm). This finding means the bearing capacity satisfies the design requirements. The *Q* - *s* curves for TP8 and TP9 are notably different than those in TP10 and TP11. For TP8 and TP9, when the load level is low, the load is linearly related to the settlement and the settlement rate increases gradually with the increase of load, while the second section shows a steep curve, which is consistent with the previous study (Fellenius et al., 2004).

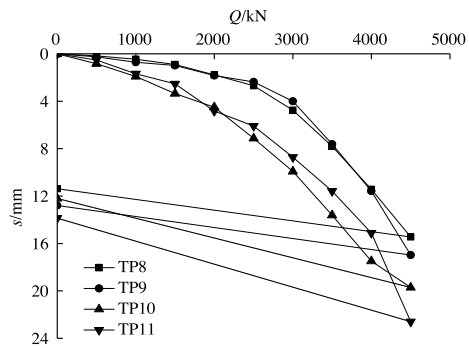

Fig. 3. Load-settlement curves for four piles.

Table 6. Results of compressive static load tests.

No.	Maximum load /kN	Settlement of pile head /mm	Springback / mm	Residual settlement /mm	Rebound ratio /%	The proportion of residual settlement to total settlement /%
TP8	4500	15.45	4.07	11.38	26.3	73.7
TP9	4500	16.98	4.19	12.79	24.7	5.3
TP10	4500	19.71	7.51	12.20	38.1	61.9
TP11	4500	22.60	8.74	13.86	38.7	61.3

For TP10 and TP11, the linear section of the curves is not obvious, and the system's curves are gentle and nonlinear. The linear section shows that the side friction is bearing the load when the load level is lower than 1500KN. With an increase in the load, the side friction becomes fully developed, and the load is borne by the strong weathered rock at the end of the pile. For TP10 and TP11, there is no straight line in the curve, which shows that the side resistance of these short piles is very small and that the pile end bears most of the vertical load. Therefore, in the design of the rock socketed short pile in weathered rock foundation, the pile head resistance should be primarily taken into account, and the side friction can be considered a safety reserve.

Calculation of Ultimate Bearing Capacity

Due to the restrictions of loading device and other factors, large diameter piles are difficult to damage in static loading tests, which means that the Q - S curve is incomplete, and the ultimate vertical bearing capacity cannot be determined directly from the curve. Predicting the ultimate vertical bearing capacity by combining the static loading test data and a reliable mathematical method is very important. The prediction models used in predicting the ultimate vertical bearing capacity are primarily the polynomial regression model, hyperbolic model, exponential model, grey theory model, empirical parameter method, and artificial neural network model design model. The exponential model, which has a high level of accuracy, was adopted in this paper.

The expression of Q - s curve can be written as

$$Q = Q_{\max}(1 - e^{-\alpha s}) \tag{1}$$

where $Q_{\max}$ is the failure load (kN) and α is subsidence attenuation factor.

The difference between the static loading test and the upper calculation is

$$\Delta Q = Q_i - Q_{\max}(1 - e^{-\alpha s}) \tag{2}$$

The overall error function is defined as

$$\varepsilon = \sum_{i=1}^{n} (\Delta Q_i)^2 \tag{3}$$

Substituting equation (2) into (3), we have

$$\varepsilon = \sum_{i=1}^{n} (Q_i - Q_{\max} + Q_{\max} e^{-\alpha s})^2 \tag{4}$$

Equation (4) is the objective function; a set of *Qmax* and α can be obtained using the DEP (variable scale optimization method) method.

Letting $(\Delta s_{i+1} / \Delta Q_{i+1}) \geq 0.10\,\text{mm/kN}$ from Equation (2), we have

$$Q_u = Q_{\max} - 10/\alpha \tag{5}$$

The predictions for the ultimate bearing capacity are shown in Table 7. Table 7 shows that the ultimate bearing capacity calculated according to concrete compressive strength of the pile body is larger than the predicted value. This finding shows that when the short pile of socketed rock reaches the ultimate bearing capacity, the concrete is not crushed, but the rock mass is destroyed. The rock socketed short pile has high safety reserve. The ultimate vertical bearing capacity does not change significantly with the increase of pile length, and the side friction has little influence on the ultimate bearing capacity. In design, the rock socketed short pile should be taken as end bearing piles. The bearing capacity cannot be improved by increasing the pile length blindly.

Table 7. Prediction results for the ultimate bearing capacity.

No.	Prediction of ultimate bearing capacity /kN	Maximum load /kN	Forecast of ultimate bearing capacity /kN	Ultimate bearing capacity calculated by strength of pile body /kN
TP8	4450	4500	6790	9668
TP9	3500	4500	6526	7542
TP10	3500	4500	5891	7542
TP11	4450	4500	6035	9668

INFLUENCING FACTORS OF BEARING CAPACITY OF ROCK SOCKETED SHORT PILES

In the paper, a FEM (ANSYS) model is adopted to simulate the short piles in weathered rock. Based on the model, the influencing factors of bearing capacity were analysed. Modelling and analysis of the single pile are performed, and a two-dimensional axisymmetric plane strain model is adopted.

The four-node straight edge quadrilateral element (PLANE42) was used for both the pile body and the surrounding rock mass, and contact units (CONTA171 and TARGE169) were arranged on the vertical plane between the pile and the soil and the pile and the rock. Coulomb friction is used to describe the interaction of the contact surfaces in this paper, and the constitutive model of rock and soil is modelled by the D-P model.

The elastic modulus of the pile is 3×10^4 MPa, and the Poisson's ratio is 0.2. The physical and mechanical parameters of each rock layer used in the simulation are shown in Table 8.

Table 8. Parameters of the soil in numerical analysis.

Soils	Thickness /m	Volumetric weight /(kN/m^3)	Poisson's ratio	Modulus of elasticity / MPa	Cohesion /kPa	Internal friction angle /(°)
Miscellaneous fill	0.40 - 6.20	17.5	0.35	5.0	/	20
Medium sand	0.50 - 5.10	20.5	0.30	16.0	/	21
Silty clay	0.50 - 8.20	19.5	0.30	12.0	20	20
Coarse sand	1.00 - 8.90	20.5	0.30	25.0	/	25
Strongly weathered granite	0.40 - 9.20	22.5	0.28	46.0	40	30
Moderately weathered granite	~	25.0	0.25	3500	50	35

Simulation Results of Static Loading Test

The results of the static loading tests of 4 rock socketed short piles carried out in Test 2 and the FEM are shown in Figure 5. Good agreement can be observed between them.

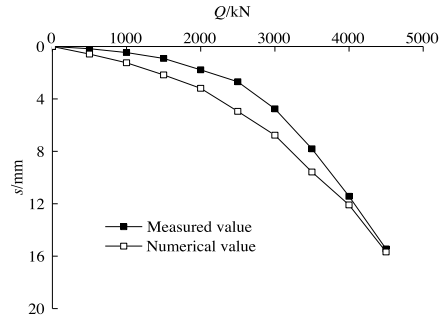

(a) TP8

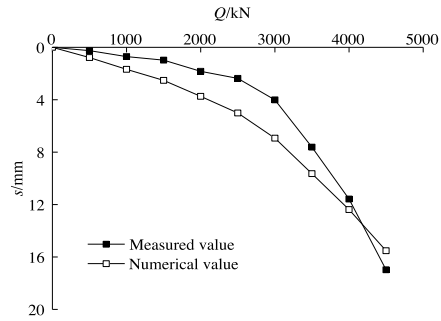

(b) TP9

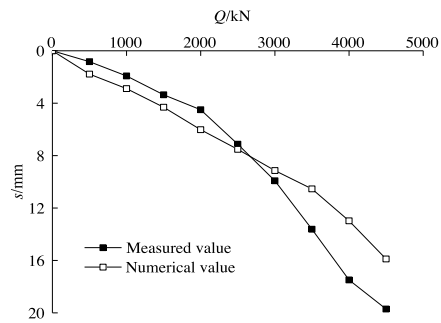

(c) TP10

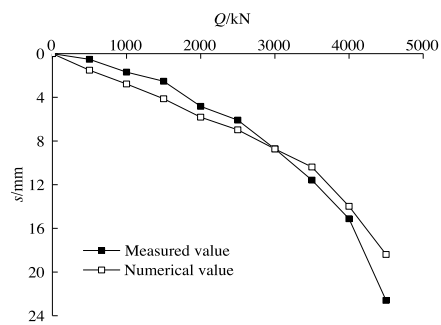

(d) TP11

Fig. 5. Comparison of load−settlement curves.

Figure 6 shows the ultimate bearing capacity obtained by a different method. It can be seen from the figure that the value obtained by the FEM is quite close to the predicted value. For TP9 and TP10, the ultimate bearing capacity is approximately 6.5MN, while for TP8 and TP11 it is approximately 7.5MN. The simulated value is approximately 1.5 times the designed value. Combining Figures 5 and 6, this shows that it is feasible to simulate the static loading tests of rock socketed short piles on weathered rock by FEM.

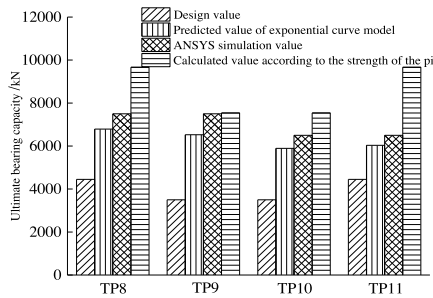

Fig. 6. The comparison of the ultimate bearing capacity of single pile.

Effect of Aspect Ratio

Assume that the pile length is L=6.0 m (L is a constant) in this paper and that the pile diameters D are taken as 800 mm, 900 m, 1000 mm, and 1200 mm, respectively. The aspect ratios L/D were 7.5, 6.7, 6, and 5, respectively. The distribution of the side friction with different aspect ratio is shown in Figure 7. Figure 7 mainly shows the change of the frictional resistance in the rock socketed section. It can be seen from Figure 7 that the peak value of the side friction gradually decreased with the increase of L/D and that the maximum value drops from 3.43MPa (L/D=7.5) to 1.34MPa (L/D=5.0). However, the location of the peak value does not change with L/D, and the position is almost unaffected by the load, which occurs at the depth of approximately 5.5 m in all cases.

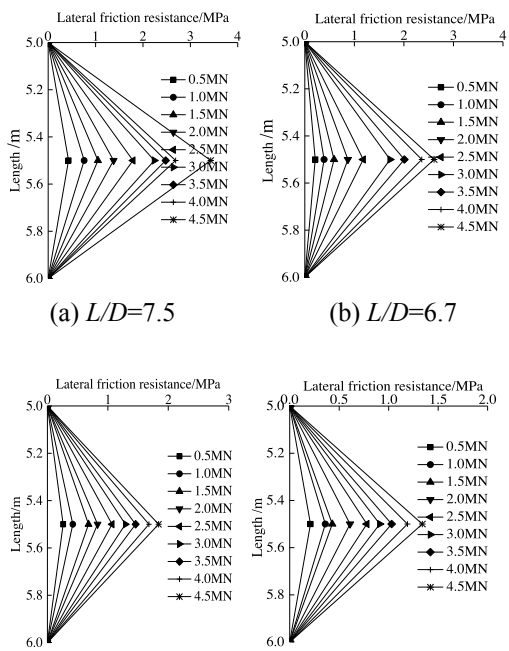

(a) L/D=7.5 (b) L/D=6.7

(c) L/D=6.0 (d) L/D=5.0

Fig. 7. Distribution of the lateral friction resistance of rock socketed piles.

Figure 8 shows the relation between the load and the settlement at the top of piles with different aspect ratios. Figure 8 shows that the *Q - s* curve is approximately linear, the settlement of pile top increases with the increase of *L/D,* and the slope of *Q - s* curve also increases with the increase of *L/D*. This is consistent with the loading characteristics of the common bored piles.

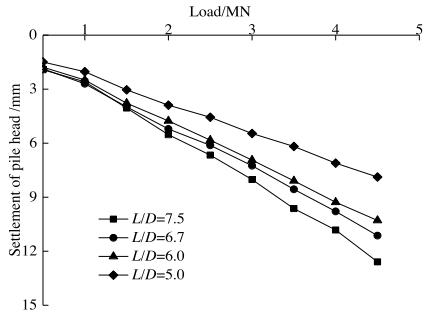

Fig. 8. *Q - s* curves of piles with different aspect ratios.

Effect of Rock Socketed Depth

To analyse the effect of rock socketed depth (h_r) on the bearing characteristics of short piles, the pile diameter *D* is assumed to be 1.0 m, and the rock socketed depth is taken as 1.0 m, 1.5 m, 2.0 m, 3.0 m, and 4.0 m. The distribution of the axial force of the pile with different rock depths is shown in Figure 9. Figure 9 shows that the attenuation law of axial force of pile body is basically the same with different rock socketed depth. The larger the rock socketed depth is, the more obvious the attenuation trend of axial force is. When $1.0D<h_r<2.0D$, the axial force shows an approximately linearly decreasing distribution, while when $2.0D<h_r<4.0D$, the axial force shows an approximately exponential decreasing distribution.

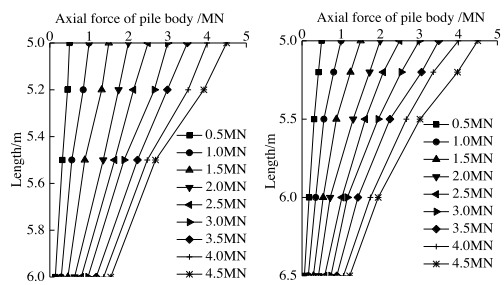

(a) h_r=1.0*D* (b) h_r=1.5*D*

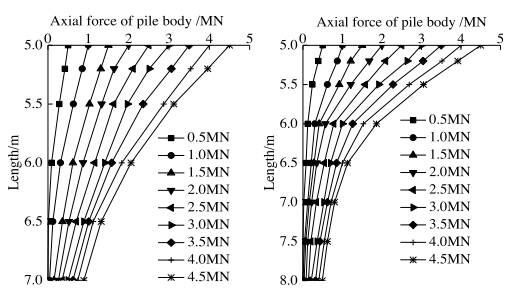

(c) h_r=2.0*D* (d) h_r=3.0*D*

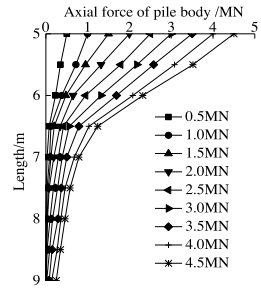

(e) h_r=4.0D

Fig. 9. Axial force distribution of piles with different rock socketed lengths.

Figure 10 shows the Q - s curves with different embedded depths in the rock. It can be seen from Figure 10 that the settlement of the pile top decreases with the increase of the rock socketed depth. When the rock socketed depth is 1.0D - 2.0D, the settlement decreases significantly, and when the rock socketed depth is 2.0D - 4.0D, the settlement is not obvious even with a changing load.

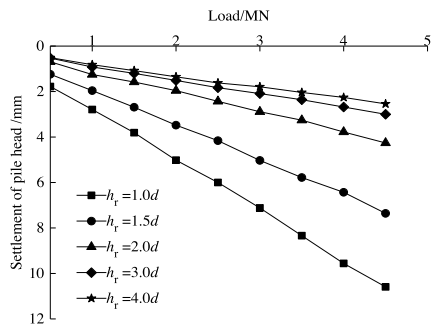

Fig. 10. Q - s curves of piles with different rock socketed lengths.

Figure 11 shows the relationship between the load and the tip resistance ratio with different rock socketed lengths. As seen from Figure 11, the pile tip resistance decreases with an increase of the rock socketed depth. The end resistance ratio of rock socketed short piles is basically within 34.4%. Combing with Figure 10, this shows that there is a critical depth in rock socketed short piles. When the rock socketed depth reaches a certain value, the bearing capacity does not obvious increase with the increase of embedded depth.

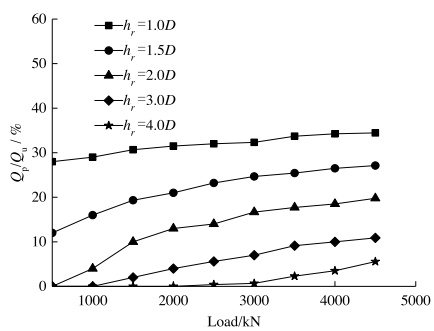

Fig. 11. Curves of relationship between load and tip resistance ratio with different rock-socketed length.

CONCLUSIONS

For a short pile embedded in strong weathered granite, whether it is a PHC pipe pile or an artificial bored pile, the ultimate bearing capacity is high, and the settlement is small, and both can meet the design requirements and have sufficient safety reserves. The ultimate bearing capacity is not obviously increased with an increase of pile length; therefore, the rock socketed short pile should be considered an end bearing pile in design. With the increase of *L/D*, the effect of end resistance is smaller. The smaller the aspect ratio is, the more the load is borne by the end of the pile. The rock pile friction peak decreases with the increase in the slenderness ratio; the pile top settlement increases with the increase of the aspect ratio; the rock socketed depth under different laws of pile axial force attenuation is largely the same; and with an increase of the depth of a rock socketed pile, the settlement decreases, and the end resistance for the bearing capacity ratio decreases.

ACKNOWLEDGMENT

The study is supported by the National Natural Science Foundation of China (51078196, 51778312), Shandong Key Research and Development Program (2017GSF16107), Shandong Provincial Natural Science Foundation of China (ZR2016EEQ08, ZR2017PEE006), Higher Educational Science and Technology Program of Shandong Province (J16LG02), and Applied Basic Research Programs of Qingdao (16-5-1-39-JCH).

REFERENCES

Armaghani, D.J., Freadonbeh, D.J., Faradonbeh, R.S. & Rezaei, H. 2016. Settlement prediction of the rock-socketed piles through a new technique based on gene expression programming. Neural Computing and Applications, **20**(2): 1-11. DOI: 10.1007/s00521-016-2618-8

Cho, C., Heo, Y. & Bae, W. 2014. Behavior Characteristics of helical pile in granite residual soil. Journal of the Korean Geoenvironmental Society, **14**(3): 41-49.

Fellenius, B.H., Harris, D.E. & Anderson, D.G. 2004. Static loading test on a 45m long pipe pile in Sandpoint Idaho. Canadian Geotechnical Journal, **41**(4): 613-628. DOI: 10.1139/t04-012

Hassan, K.M. & O'Neill, M.W. 1997. Side load-transfer mechanisms in drilled shafts in soft argillaceous rock. Journal of Geotechnical and Geoenvironmental Engineering, **123**(2): 145-152. DOI: 10.1061/(ASCE)1090-0241(1997)123:2(145)

Kwon, O.K., Kim, J.B. & Kweon, H.M. 2014. An experimental study on the resistance and movement of short pile installed in sands under horizontal pullout load. International Journal of Naval Architecture and Ocean Engineering, **6**(1): 87-97. DOI: 10.2478/ijnaoe-2013-0165

Leong, E.C. & Randolph, M.F. 1994. Finite element modeling of rock-socketed piles. International Journal for Numerical and Analytical Methods in Geomechanics, **18**(1): 25-47. DOI: 10.1002/nag.1610180103

Madhusudhan, B.N., Baudet, B.A. & Ferreira, P.M.V. 2017. Performance of fiber reinforcement in completely decomposed granite. Journal of Geotechnical and Geoenvironmental Engineering, **143**(8): 04017038. DOI: 10.1061/(ASCE)GT.1943-5606.0001716

Musarra, M. & Massad, F. 2015. Static load tests in an instrumented rock socket barrette pile. Soils and Rocks, 38(2): 163-177.

Rowe, R.K. & Armitage, H.H. 1987. Theoretical solutions for axial deformation of drilled shafts in rock. Canadian Geotechnical Journal, **24**(1): 114-125.

Xia, X., Li, H.B. & Li, J.C. 2013. A case study on rock damage prediction and control method for underground tunnels subjected to adjacent excavation blasting. Tunnelling and Underground Space Technology, **35**: 1-7. DOI: 10.1016/j.tust.2012.11.010

Submitted: 01/10/2017
Revised: 30/04/2018
Accepted: 06/05/2018

دراسة خصائص قدرة التحمل لركائز قصيرة صخرية مخروطية في موقع الصخور المجوفة

***لي شين يوان، باي شياو يو وتشانغ مينغ يي**
*كلية الهندسة المدنية، جامعة شوتشو للتكنولوجيا، شوتشو، الصين
كلية الهندسة المدنية، جامعة تشينغداو للتكنولوجيا، تشينغداو، الصين

الخلاصة

تم دراسة سلوك التحمل وميكانيكية انتقال الحمل في الركائز القصيرة الصخرية المخروطية عن طريق الفحص وتطبيق FEM على حالتين مختلفتين من 11 ركيزة قصيرة في أساس مصنوع من الصخور المجوفة في مدينة تشينغداو. تمت مناقشة تأثيرات نسبة الأبعاد وطول الصخور المخروطية على سلوكيات التحمل للركائز بواسطة تطبيق FEM. وأشارت النتائج أن قدرة التحمل القصوى لتلك الركائز كانت أعلى، والتسوية كانت أصغر، مما يعني أنها يمكن أن تلبي المتطلبات الهندسية وأن لها احتياطيات أمنية عالية. علاوة على ذلك، لا يمكن ملاحظة حدوث تغيير في قدرة التحمل القصوى بسهولة عند زيادة أطوال الركائز، مما يدل على أن الـ 11 ركيزة لديها خصائص اسناد نهائي قوية. يتناقص الاحتكاك الجانبي لقمة الركائز مع زيادة نسبة الأبعاد كما هو الحال مع هبوط قمة الركيزة. في ظل وجود أطوال مختلفة من الصخور، تكون معادلة التوهين للقوة المحورية ثابتة؛ ويتناقص هبوط قمة الركيزة مع زيادة طول الصخور المخروطية، وتقل نسبة المقاومة الأساسية لقدرات التحمل مع زيادة الطول. نتائج البحث يمكن أن توفر مراجع لتصميم ركيزة قصيرة صخرية مخروطية في ظل ظروف جيولوجية مماثلة.